

REACTOR OPERATOR COMPANION FOR CANDU HEAT TRANSPORT SYSTEMS

W.J. Garland*, J. Anderson** and J.D. Hoskins*

*Department of Engineering Physics, McMaster University
Hamilton, Ontario

**Atomic Energy of Canada Ltd., CANDU Operations
Mississauga, Ontario

ABSTRACT

The use of an "Operator Companion", an expert system which can monitor and assess the current status of a power plant, has been proposed by AECL to assist in the operation of a CANDU reactor. A number of satellite expert systems, each monitoring a specific system of a power plant, are to be interfaced with the operator companion or main expert system.

As a step in the development of a complete operator companion system, work has begun on the development of a satellite system for the heat transport system of a CANDU nuclear reactor. This will consist of four parts: (1) a heat transport system simulator, (2) a trend analyzer, (3) an expert system, and (4) a data acquisition system.

Work is progressing on the simulator portion of the satellite expert system. It will encompass steady state equations for calibrations and fingerprinting purposes as well as transient calculations to enhance trend analysis.

Presented at the 14th Annual Nuclear Simulation Symposium, 1988 April 25-26,
Pinawa, Manitoba.

1.0 INTRODUCTION

1.1 OPERATOR COMPANION

The use of a number of satellite expert systems each cooperating with a central, main expert system is the route being pursued by Atomic Energy of Canada Limited [NAT87] for the construction of an Operator Companion aimed at assisting the operation of a nuclear power plant (see Figure 1.1).

The design and implementation of any expert system for monitoring and, eventually, controlling complex plants should adhere to the following guidelines:

- (1) the system's knowledge must be accessible and comprehensible to both diagnostic experts and plant operators;
- (2) the system should be constructable incrementally as expertise and manpower become available;
- (3) the system will grow to a large size, so attention must be paid to structuring the system in such a way that real-time operation at a future date is not jeopardized.

These aspects are particularly important when dealing with a society of expert systems which are to be integrated into a single global system for monitoring plant operations and providing advice to the operator. In view of the above guidelines, the heat transport system was chosen for the initial investigation.

This work discusses the simulation and trend-analysis aspects of a satellite expert system for the main heat-transport system in the CANDU nuclear power station (see Figure 1.1). The satellite expert system, itself, is also discussed to the extent that it impacts on the simulator and the trend analyzer.

1.2 SATELLITE SYSTEM FOR CANDU HTS

The use of an "Operator Companion", an expert system with the purpose of monitoring and assessing the current status of a power plant, has been proposed by AECL to assist

in the operation of a CANDU nuclear reactor. The operator companion or main expert system would be interfaced with a number of satellite expert systems, each monitoring a different component of a reactor. As a step in the development of a complete operator companion system, the development of a satellite system for the heat transport system of a CANDU nuclear reactor was investigated. The satellite is to consist of four parts: (1) a data acquisition system, (2) a trend analyzer, (3) an expert system, and (4) a heat transport system simulator.

In any heat transport system, one of the most serious events is a loss-of-coolant accident or LOCA. Thus, one of the primary functions of the satellite is to identify the presence of a LOCA in the heat transport and associated systems as well as diagnose the size and location of the leakage. Leakages are classified by the actual failure mode

- (a) internal leakages through valves associated with the Pressure and Inventory Control System causing transfer of inventory from one vessel to another;
- (b) external leakages from HT and associated systems into the reactor building;
- (c) leakages into secondary side of heat exchangers employed in the HT and associated systems.

Class (a) leakages are specific to the PIC system and do not result in a loss of coolant from the system. This type of leakage is outside of the domain of the satellite system, requiring an expert system of its own. The satellite system will have to differentiate between external and internal leakages but will only do a more detailed analysis for the external leakage case. Class (b) and class (c) both involve a loss of coolant from the heat transport system and the analysis is similar for each of them. It is possible to differentiate between them by the detection of D_2O on the secondary side for class (c) leakages versus the detection of D_2O or high pressure in the containment. The discussion will be based on external leakages in general.

2.0 COMPONENTS OF THE SATELLITE SYSTEM

2.1 DATA ACQUISITION

Returning to Figure 1.1, there is a flow of information from the reactor to the data acquisition system. This information would include the D₂O levels in the PIC vessels, pressures and temperatures needed for mass inventory calculations and for simulation purposes, and alarms (for example, beetle alarms which detect moisture outside of the HTS loops). This raw information is passed to the trend analyzer for processing.

2.2 TREND ANALYZER

The trend analyzer observes trends on the order of seconds (as in the case of D₂O levels where any deviation may suggest an abnormal event), minutes, hours or even months. This allows us to identify any deterioration or problems of high frequency within the heat transport system, building up a history of the reactor. To detect deviation, a base line is of course necessary. Hence the trend analyzer consists of a data storage section (time slice snapshots) and steady state calibration.

2.3 EXPERT SYSTEM

An expert system provides the "brains" of the satellite, applying rules to information provided by the trend analyzer in order to identify any abnormal event in the heat transport system. If such an event is detected, appropriate messages are sent to the main expert system and a simulation is invoked to provide the operator with details specific to the event(s). The expert system could also receive commands from the operator companion to check the HTS status or to simulate the effect of any action the operator may want to take.

2.4 SIMULATOR

The final component of the satellite system is a simulator. It consists of two portions. The first portion performs calculations specific to small LOCA analysis. These would include

calculations of mass inventory and rate of leakage, estimation of D₂O storage tank drainage time and reactor trip time, overall heat balance and any other pertinent calculations. The second part is a somewhat crude simulation of the heat transport system. It involves a rate form of the equation of state, solved simultaneously with conservation equations of mass, momentum and energy. This leads to a matrix equation of the form

$$\frac{d\mathbf{U}}{dt} = \mathbf{A} \mathbf{U} + \mathbf{B}$$

where \mathbf{U} is a vector containing the mass, enthalpy, and pressure of each node and the flow in each link. \mathbf{A} and \mathbf{B} are known matrices derived from the conservation equations and equation of state.

3.0 MASS INVENTORY METHODOLOGY

By observing the manner in which the mass inventory of the vessels contained in the PIC system (D₂O storage tank, pressurizer, and degasser condenser) are changing, it is possible to identify that there is an external leakage (LOCA) in the loop and estimate the rate of leakage. Additional information of interest to the operator concerning these vessels is the estimation of time for drainage of the D₂O storage tank and time to the reactor trip setpoint in the pressurizer [AN87].

In order to derive the necessary relations for LOCA analysis, it is necessary to determine how the PIC system responds to various sizes of leakage rate. Five ranges of leakage rate can be identified for the mass inventory methodology. These are summarized in Figures 3.1 through 3.5.

(i) Category A (Figure 3.1)

The smallest size corresponds to a "drip". There is no noticeable change in the HTS parameters and therefore, no action is taken by the PIC system. Only through a beetle alarm

can this size of leak be identified. No immediate action would be taken by the operator, except to have it investigated as a maintenance problem.

(ii) **Category B (Figure 3.2)**

The next rate size of D₂O leakages extends from the smallest leakage rate for which the PIC system would respond to a rate equal to the capacity of the feed pumps. After an initial transient of pressurizer level and HT pressure, mass inventory in the HT loop would be maintained through the feed pumps only. The feed pumps would remove D₂O from the storage tank at a rate equal to the leakage rate. Once the storage tank has drained, D₂O would be removed from the pressurizer at a rate equal to the leakage rate. Thus the change in tank levels give an estimate of the leak rate. The time to reactor trip is estimated to be the time for the storage tank to drain added to the time for the pressurizer inventory to decrease to the setpoint level from its current level, assuming a constant leakage rate until reactor trip occurs. This is not necessarily accurate since as the pressurizer level decreases, the pressurizer cannot maintain pressure and inventory in the HT system and the leak rate will decrease. Thus, the initial leak rate estimate is a conservative one. After the storage tank has drained it is necessary to estimate the change of mass inventory (dM_{loop}/dt) in the HT loop in order to obtain the leakage rate. This can be done by utilizing the equation of state, discussed in Section 4.

$$\frac{dP}{dt} = \left(F_1 \frac{dM_{loop}}{dt} + F_2 \frac{dH}{dt} + F_3 \frac{dV}{dt} \right) / (F_4 M_g + F_5 M_f) \quad (3.1)$$

In this equation, dV/dt is equal to zero, dP/dt is measured and M_f , M_g , F_i are taken from nominal values. Rearranging, we obtain

$$\frac{dM_{loop}}{dt} = \frac{1}{F_1} \left[(F_4 M_g + F_5 M_f) \frac{dP}{dt} - F_2 \frac{dH}{dt} \right] \quad (3.2)$$

where

$$\frac{dH}{dt} = W_s h_s + W_f h_f - W_L h_L$$

The flow W_L is the leakage rate and h_L is the enthalpy at the leak location. The subscripts s and f represent surge and feed respectively. Comparing the changes in inventory, we observe

$$-\frac{dM_{PIC}}{dt} - W_L = \frac{dM_{loop}}{dt} \quad (3.3)$$

Substituting (3.2) into (3.3) and solving for W_L ,

$$W_L = \frac{\left[-(F_4 M_g + F_5 M_f) \frac{dP}{dt} - F_1 \frac{dM_{PIC}}{dt} + F_2 (W_s h_s + W_f h_f) \right]}{(F_2 h_L + F_1)} \quad (3.4)$$

It should be noted that only one feed pump may be operating initially. Thus the upper limit of this range increases from the capacity of one feed pump operating to the capacity of two feed pumps operating when the operator switches on the second pump.

(iii) Category C and Category D (Figures 3.3 and 3.4)

Beyond the capacity of the feed pumps, the inventory in the HT loop cannot be maintained by the feed pumps alone. A net loss in inventory in the HT loop causes a decrease in the pressure within the loop causing the pressurizer to inject D_2O into the system. The leakage rate is estimated from equation (3.4). The time to reactor trip is estimated using the current rate of change of pressurizer inventory. If the leakage rate were constant, this rate of change would also be expected to be approximately constant. However, since the pressure in the loop cannot be maintained the leakage rate will decrease and, therefore, the rate of change of pressurizer inventory will decrease. The actual trip time would be longer than the estimated value. The calculated time would be a worst case estimation.

For a certain leakage rate (RTD), the D_2O storage tank will drain at the same time as the pressurizer level reaches the trip setpoint. For leakage rates greater than RTD (category D), reactor trip occurs before the storage tank drains and the trip time is based simply on the rate of change of pressurizer inventory. For the range greater than the feedpump capacity and less than RTD, the trip time is estimated to be the time to D_2O storage tank drainage plus the time for the pressurizer level to decrease to the trip level subsequent to storage tank

depletion. The rate change of inventory in the pressurizer used in this calculation is assumed to be the current rate of change. As explained previously, the trip time would be a worst case estimation.

(iv) Category E (Figure 3.5)

Beyond some leakage rate RMAX, the satellite system is unable to respond quickly enough to be of much use during a loss-of-coolant accident. Reactor trip may occur within a couple of minutes after identification of the event, based on the pressurizer setpoint or on pressure or temperature alarms in other parts of the reactor. Augmenting the LOCA analysis through a simulation (described in Section 4.0) may prove necessary in order to make the limiting rate RMAX (the upper limit of category D) as large as possible i.e., to extend the useful range of the satellite expert system.

The mass inventory of the degasser condenser has not been included in the above discussion. It does not serve to replace inventory during a LOCA and does not trigger any alarms. Therefore no analysis is done which is specific to this vessel except that any change of inventory in the vessel is included in the calculation for the total loss of inventory from the PIC system. This compensates for internal leakages which may involve, for example, the transfer of D₂O from the degasser condenser to the D₂O storage tank caused by the spurious opening of a degasser condenser level control valve.

The D₂O recovery system must also be included in the analysis of a LOCA. This system, initially, does not have an effect on the analysis until the recovery tank is 95% full. At this time, the recovery pumps switch on and return the D₂O to HTS via the feed pumps. This has the effect of reducing the rate at which D₂O is taken from the D₂O storage tank and therefore, prolonging the time to drainage of the storage tank. The recovery pumps will remain on until the recovery tank is only 45% full and then switch off until the 95% mark is once again reached. This assumes that the operator has switched the recovery pumps to automatic mode when the external leakage was first identified. The calculation of the

leakage rate will include the addition of the flow rate between the recovery tank and the feed pumps to the total loss of inventory from the PIC system. The calculation of reactor trip time and storage tank drainage time will not be altered. However, another time estimation of possible interest to the operator can be identified. This is estimation of time to recovery pumps on or, if the pump is currently operating, time to recovery pump off.

The above calculations for LOCA analysis are carried out in the simulator components of the satellite system, although they are independent of the simulation itself. Mass inventory calculations for each vessel are done on a continuous basis. The level of each vessel is converted to a volume by assuming that the vessel is cylindrical with hemispherical ends (horizontal for D₂O storage tank, vertical for pressurizer and degasser condenser). This assumption is common to other simulators (e.g. FIREBIRD).

4.0 SIMULATOR

Transient calculations, intended to enhance trend analysis of the heat transport system, are to be performed using the conservation equations for mass, momentum and energy, and the rate form of the equation of state [GA87a,b].

Figure 4.1 shows a typical nodal layout of a CANDU nuclear reactor. A given node, i , is described by an enthalpy, H_i , a mass M_i , and a pressure P_i . Each link has a corresponding flow, W_j , associated with it. A vector U can be defined, containing the enthalpy mass and pressure values of the nodes and the flows through each link:

$$U = \{W_1, W_2, \dots, P_1, P_2, \dots, M_1, M_2, \dots, H_1, H_2, \dots\}$$

In general, the task is to solve the matrix equation,

$$\frac{dU}{dt} = AU + B, \quad (4.1)$$

over the time domain of interest. The matrices A and B are taken from the conservation equations and the equation of state, summarized below.

$$\text{mass:} \quad \frac{dM_i}{dt} = \sum_j W_j \quad (4.2)$$

$$\begin{aligned}
\text{momentum: } \frac{dW_j}{dt} = \frac{A_j}{L_j} & \left[(P_{ie} - P_{ix}) - \left(\frac{f_j L_j}{D_j} + K_j \right) \frac{|W_j| W_j}{2 \rho_j A_j^2} \right] \\
& + \frac{A_j}{L_j} h_j \rho_j g + \frac{A_j}{L_j} \Delta P_{\text{pump}j}
\end{aligned} \tag{4.3}$$

$$\text{enthalpy: } \frac{dH_i}{dt} = \sum_{v_{in}} W_v \left(\frac{H_v}{M_v} \right) - \sum_{v_{out}} W_v \left(\frac{H_v}{M_v} \right) + Q_i \tag{4.4}$$

$$\text{equation of state: } \frac{dP_i}{dt} = \frac{F_1 \frac{dM_i}{dt} + F_2 \frac{dH_i}{dt} + F_3 \frac{dV_i}{dt}}{M_g F_4 + M_f F_5} \tag{4.5}$$

Flow is recognized as the most important dependent parameter [PO71]. Fully implicit treatment of flow was found to lead to excellent numerical stability, consistency and convergence for rate form of the equation of state [GA87b]. Incorporating an implicit pressure dependence in the numerical method gave a further dramatic improvement in numerical stability. It was observed that there is no need to treat mass and enthalpy terms implicitly since the implicit contributions cancelled out, at least in the simple case of two nodes joined by a link. Thus, the mass and enthalpy are calculated after the flow is updated:

$$\mathbf{M}^{t+\Delta t} = \mathbf{M}^t + (\mathbf{A}^{MW} \mathbf{W}^{t+\Delta t} + \mathbf{B}^M) \Delta t \tag{4.6}$$

$$\mathbf{H}^{t+\Delta t} = \mathbf{H}^t + (\mathbf{A}^{HW} \mathbf{W}^{t+\Delta t} + \mathbf{B}^H) \Delta t \tag{4.7}$$

Performing the implicit calculation of flows first, the updated flows, $\mathbf{W}^{t+\Delta t}$, can be used to update mass and enthalpy.

To update the flows, the matrix equation is reduced to a form containing only flows and pressures. To solve pressure implicitly, equation (4.5) must be in terms of W_j . Substituting for dM_i/dt and dH_i/dt and setting dV_i/dt equal to zero,

$$\begin{aligned} \frac{dP_i}{dt} = & - \sum_{j_{in}} \left[C_{1i} + C_{2i} \frac{H_i}{M_i} \right] W_j \\ & + \sum_{j_{out}} \left[C_{1i} + C_{2i} \frac{H_i}{M_i} \right] W_j \end{aligned} \quad (4.8)$$

where

$$C_{1i} = \frac{F_1}{M_g F_4 + M_f F_5}$$

$$C_{2i} = \frac{F_2}{M_g F_4 + M_f F_5}$$

In matrix notation:

$$\begin{bmatrix} \dot{\mathbf{W}} \\ \dot{\mathbf{P}} \end{bmatrix} = \begin{bmatrix} \mathbf{A}^{WW} & \mathbf{A}^{WP} \\ \mathbf{A}^{PW} & 0 \end{bmatrix} \begin{bmatrix} \mathbf{W} \\ \mathbf{P} \end{bmatrix} + \begin{bmatrix} \mathbf{B}_W \\ \mathbf{B}_P \end{bmatrix} \quad (4.9)$$

where, for a simple circular loop of L links and N nodes:

$$\mathbf{A}^{WW} = \begin{pmatrix} -k_1 W_1 & & & & \\ & & & & 0 \\ & & & & \\ & & -k_2 W_2 & \dots & \\ & 0 & & & -k_L W_L \end{pmatrix} \quad (4.10)$$

$$\mathbf{A}^{WP} = \begin{pmatrix} \frac{A_1}{L_1} & -\frac{A_1}{L_1} & & & \\ & \frac{A_2}{L_2} & -\frac{A_2}{L_2} & & \\ & & & \dots & \\ & & & & \frac{A_L}{L_L} \\ -\frac{A_L}{L_L} & & & & \end{pmatrix} \quad (4.11)$$

$$\mathbf{B}_W = \begin{bmatrix} \frac{A_1}{L_1} (h_1 \rho_1 g + \Delta P_{\text{pump}_1}) \\ \vdots \\ \vdots \\ \vdots \\ \vdots \end{bmatrix} \quad (4.12)$$

$$\mathbf{A}^{PW} = \begin{bmatrix} -(C_{11} + C_{21} h_1) & +(C_{11} + C_{12} h_1) & 0 & 0 \\ 0 & -(C_{12} + C_{22} h_2) & (C_{12} + C_{22} h_2) & 0 \\ \vdots & \vdots & \vdots & \vdots \\ \vdots & \vdots & \vdots & \vdots \\ (C_{1N} + C_{2N} h_N) & 0 & 0 & -(C_{1N} + C_{2N} h_N) \end{bmatrix} \quad (4.13)$$

Now, since

$$\dot{\mathbf{P}} = \mathbf{A}^{PW} \mathbf{W} + \mathbf{B}_P, \quad (4.14)$$

We can substitute this into the flow equation to give:

$$\begin{aligned} \dot{\mathbf{W}} &= \mathbf{A}^{WW} \mathbf{W} + \mathbf{A}^{WP} \mathbf{P} + \mathbf{B}_W \\ &= \mathbf{A}^{WW} \mathbf{W} + \mathbf{A}^{WP} (\mathbf{P}^t + \Delta t \mathbf{P}) + \mathbf{B}_W \\ &= \mathbf{A}^{WW} \mathbf{W} + \mathbf{A}^{WP} (\mathbf{P}^t + \Delta t \mathbf{A}^{PW} \mathbf{W} + \Delta t \mathbf{B}_P) \end{aligned} \quad (4.15)$$

Setting

$$\dot{\mathbf{W}} = \frac{\mathbf{W}^{t+\Delta t} - \mathbf{W}^t}{\Delta t} \quad \text{and} \quad \mathbf{W} = \mathbf{W}^{t+\Delta t},$$

the implicit solution is given by:

$$\begin{aligned} [\mathbf{I} - \Delta t \mathbf{A}^{WW} - \Delta t^2 \mathbf{A}^{WP} \mathbf{A}^{PW}] \mathbf{W}^{t+\Delta t} \\ = \mathbf{W}^t + \Delta t \mathbf{A}^{WP} \mathbf{P}^t + \Delta t^2 \mathbf{A}^{WP} \mathbf{B}_P + \Delta t \mathbf{B}_W. \end{aligned} \quad (4.16)$$

A slight improvement on this can be obtained by perturbing the $\mathbf{K} \mathbf{W}^2$ term to yield:

$$\begin{aligned}
& [\mathbf{I} - 2K\Delta t - \Delta t^2 \mathbf{A}^{WP} \mathbf{A}^{PW}] \mathbf{W}^{t+\Delta t} \\
& = \mathbf{W}^t - \Delta t \mathbf{A}^{WW} \mathbf{W}^t + \Delta t \mathbf{A}^{WP} \mathbf{P}^t + \Delta t^2 \mathbf{A}^{WP} \mathbf{B}_P + \Delta t \mathbf{B}_W.
\end{aligned} \tag{4.17}$$

After solving equation (4.16) or (4.17) for the new flows, the pressures are updated using

$$\mathbf{P}^{t+\Delta t} = \mathbf{P}^t + \Delta t \mathbf{A}^{PW} \mathbf{W}^{t+\Delta t} \tag{4.18}$$

The masses and enthalpies are updated using equations (4.6) and (4.7) as mentioned earlier.

One problem with this approach is that the pressure may drift away from a value consistent with the mass and energy [GA87b]. The problem can be surmounted by using a feedback mechanism:

$$\mathbf{P}^{t+\Delta t} = \mathbf{P}^{t+\Delta t} + \frac{h^t - h_{\text{calc}}}{dh/dp} * \text{ADJ} \tag{4.19}$$

where ADJ is an adjustment factor $\in [0,1]$, to allow experimentation with the amount of feedback. This adjustment is equivalent to 1 iteration on P, given ρ and h , and is done automatically by the water property subroutines. Typically, setting $\text{ADJ} = 0.5$ gave good results.

The scheme has been shown to be very robust and stable for a simple 2 node-1 link case for two phase and single phase flow, including void collapse. Large time steps (tens of seconds) give stable answers that are asymptotically correct. The scheme will track pressure waves and waterhammer when sufficiently small time steps are used.

5.0 TREND ANALYZER

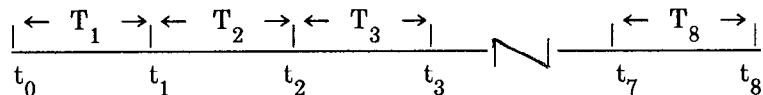
As discussed in section 2.2, the role of the trend analyzer is to observe trends as they develop in the heat transport system. To this end, a scheme for the detection of the operating state and a data storage scheme are investigated.

5.1 MOVING AVERAGES

In order to monitor power, the various flows, pressures, and temperatures for trend analysis, measurements must be taken on a continuous basis. However, this implies that hundreds of measurements must be recorded. This is unrealistic if, for example, the trend

analysis was to span a period of one year. Since we are interested in the behaviour of operating parameters (flow rate, temperature, etc.) over time, it is more plausible to analyze the averages of variables taken at different time intervals.

In order to state a mathematical relationship for computing moving averages, consider the following time axis:



where t_i = time [seconds], $i = 0, 1, \dots, 8$

T_j = time interval [seconds], $j = 1, 2, \dots, 8$.

Note that measurements are recorded on a continuous basis but the averages are computed at time t_i . The choice of limiting the axis to t_8 may be explained as follows : to analyze trends for one year a convenient time scale is needed, and for reasons which will be stated shortly, this scale is chosen to be in powers of ten (10), i.e. $t_0 = 0$ sec., $t_1 = 10$ sec., ... $t_8 = 10^8$ sec. which is roughly one year. Now, the measurement made at time t_0 is in itself an average since it is the only measurement; however, at time t_1 the average is :

$$A_1 = \frac{\Sigma(\text{pts})_1}{N_1} \quad (5.8)$$

where A_1 = average of measurements in time interval 1 (T_1)

N_1 = number of measurements recorded in T_1

$\Sigma(\text{pts})_1$ = sum of measurements recorded in T_1 .

Therefore at time t_1 a comparison could be made between the initial measurement taken at t_0 and the average A_1 . Now, the average from t_0 to the end of t_2 , for instance is calculated as follows :

$$\text{Ave. } t_0 \text{ to } t_2 = \frac{N_1 A_1 + N_2 A_2}{N_1 + N_2} \quad (5.9)$$

Note that this does not represent A_2 which is the average of measurements taken between t_1 and t_2 only. Substituting for A_1 from equation (5.8) into equation (5.9), the following result is

obtained :

$$\text{Average from start to end of interval 2} = \frac{\Sigma(\text{pts})_1 + \Sigma(\text{pts})_2}{N_1 + N_2} \quad (5.10)$$

Generalizing

$$\text{Average from start to end of interval } i = \frac{\Sigma(\text{pts})_1 + \Sigma(\text{pts})_2 + \dots + \Sigma(\text{pts})_i}{N_1 + N_2 + \dots + N_i} \quad (5.11)$$

for $i \leq 8$.

This expression requires only the number of measurements and their sum within each interval. It was for this reason that time slices of 10^j seconds, $j = 0,1,\dots,8$, were chosen. Only nine (9) intervals of a parameter would have to be analyzed to cover a period of one year (instead of hundreds)! This time scale is quite appropriate since steady state takes about 15 minutes to reach. Hence the first four (4) moving averages are analyzed within 16 minutes while the remaining five (5) averages essentially span the entire one year period. Note that each interval (slice) is important for assigning confidence levels as discussed in section 5.2 as well as for keeping the analysis in focus.

In order to understand how the concept of Moving Averages (i.e. Time Slices) works, figure 5.1 illustrates a flowchart which computes averages for certain time periods over a one year range. The basis of the flowchart in figure 5.1 can be best explained by referring to figure 5.2 which shows the distribution of time slices. Except for register A which can only contain one measurement (the most recent one), registers B through I (inclusive) are subdivided into ten (10) bins and contain one (1) value per bin.

To begin, consider registers A, B, and C. Register A contains only the most recent measurement and hence it is updated every second, as well as being an average in itself. At time zero, all bins are empty so that when one second has elapsed A has a value. After two seconds, A contains a new measurement and the previous one gets bumped into bin 1 of register B. The average of register B at this particular instant is simply the value in bin 1. Now after three seconds, A has the latest data, the previous bin 1 value of B gets shifted into bin 2 of B, the previous A value (i.e. after 2 seconds) jumps down into bin 1 of B, and a new

average for register B is computed. This process continues until all ten bins of B are filled. At this instant, the newest average of register B jumps down into bin 1 of register C. Then, when A gets the next value, bin 10 of B is discarded as everything shifts to the right to accommodate the incoming previous A value. To summarize, register A contains only one bin which is updated every second, register B contains ten bins and each is updated every second, and register C contains ten bins with each one being updated every ten seconds since it is dependent on the time width of register B. Note that whenever a bin of a register is updated, a new average for the register is calculated. As a result there are only nine values which characterize a parameter, i.e. from start to 1 sec., from 1 sec. to 10 sec., from 10 sec. to 100 sec., and so on. The entire process just described is applicable through to register I. Note also that the above discussion assumes a sampling rate of one per second. However this rate is arbitrary since the shifting and updating of bins, as well as the computation of a register's average is dependent on bin status (i.e. counting statistics) rather than on time.

The advantage of using time slices is that 10^8 measurements for one parameter need not be kept, which is impractical considering that there are perhaps several hundred parameters to be monitored. Since there are eight registers with ten bins and one register with only one bin, only 81 values spanning one year need be kept for a parameter. Obviously this is much more efficient than maintaining 10^8 samples! In figure 5.1 the boxed outline shows that the same type of flow is common to regions B through I (inclusive). Finally, when the one year average is computed, it can be stored for comparison purposes, i.e. to the following yearly average.

5.2 DATA ANALYSIS

The information that the trend analyzer supplies to the satellite expert system can be grouped into three categories.

The first is the collection of current parameter values and averages for the previously measured values, as discussed in Section 5.1. In register A, the current value for HTS

pressures, temperatures etc. are stored. In register B, the last 10 measurements are stored covering, say, the previous 10 seconds. In register C, the last 10 averages (of 10 seconds each) are stored, covering the last 100 seconds. In register D, the last 10 averages (of 100 seconds each) are stored, covering the last 1000 seconds, and so on. This is the basic data used by the trend analyzer and other portions of the companion.

The second category of information is the status flag for each parameter in each register. In each register this flag denotes the comparison of the value in the first bin of that register to the average of the register. The value of the flag can vary from -100 to $+100$ to indicate the range: very much less than the average (-100) to very much greater than the average ($+100$). From this flag, we can get a quick picture of any transient or some measure of the degree to which the system is at steady state. For instance, a flag value of 0 in register B for ROH pressure shows that the current value of the pressure is the same (to within the set tolerance) as the average over the last 10 seconds. This is a strong indication that no major transient is underway. The addition of these flags is a small overhead for the information and power gained.

The third category of information contains the results of the heat balance check that is to be performed at each sample interval. The primary and secondary power are compared. If they agree with each other, this is a strong indication that a) steady state exists and b) no calibration or measurement errors exist for the parameters involved. If they do not agree, then either (a) or (b) or both are not true. Two status flags would indicate the confidence (-100 to $+100$) that (a) or (b) are true. The flag status of each register (discussed above) would be used to adjust the confidence level for condition (a) or (b). For example, if any parameter has its B register flag non-zero, we can be more confident that (a) is not true (ie. not a steady state) but we cannot improve on our estimation of (b) with this new information. If all but a few parameters have zero-flags, this indicates a measurement error, increasing our confidence that (b) is not true.

With the above scheme, the trend analyzer can:

- (1) routinely and continuously monitor the HTS;
- (2) store all pertinent information in a finite set;
- (3) perform base level calculations to infer plant status (steady state or not, measurement/calibration errors or not);
- (4) and provide convenient flags that the rest of the reactor operator companion, especially the satellite expert system can use.

The next section indicates how an expert system might utilize such information.

6.0 SATELLITE EXPERT SYSTEMS

The satellite expert system receives input from the trend analyzer on the status of the heat transport system (pressures, temperatures, levels, alarms, calibration information, etc.), from the simulator (inventory and transient simulations) and from the main expert system (status of other systems and operator input). The primary function of the satellite expert system is to monitor this information and deduce any significant occurrences such as a LOCA, reactor trip, etc. and the severity of the incident (small or large break, etc.). The satellite expert system is presently conceived to monitor a limited number of indicators for making initial diagnosis and to initiate further investigations when supporting evidence is needed to substantiate a hypothesis.

Further, the expert system should exhibit advanced features, including the ability to review diagnoses with operator driven changes (what-if analysis), to explain how a conclusion was reached, to interact with existing databases for operating procedures, and to read and write to a common "blackboard". The system must accommodate growth by allowing easy updates to rules and system structure and by having an upward migration path to larger and faster machines. Initial work is to be implemented on a personal computer.

McMaster University has received a site license for Personal Consultant Plus (Texas Instruments) which operates on an IBM AT or compatible. This LISP based code has all of the required features.

6.1 LOCA DETECTION

As an example of how a satellite expert system for LOCA detection might be set up, consider a system based on the monitoring of:

- 1) the beetle moisture detectors;
- 2) the ROH pressure;
- 3) the PIC inventory;
- 4) the surge tank level;
- 5) the containment pressure;
- 6) the overall status of the trend analyzer.

It is assumed that the moisture detectors are of the ON/OFF type and the other parameters are multi-valued (ok, low, dropping, etc.).

A table, such as Table 6.1, is constructed by the Knowledge Engineer in consultation with human experts. A typical consultation might be:

KE: What system behaviour would indicate a LOCA of size C?

EXPERT: The moisture alarms would go off, the ROH pressure would drop and continue to drop, the PIC inventory would be low, the surge tank level would be dropping slowly, the containment pressure would probably be a bit high and the trend analyzer would show abnormalities. Of course, these are not firm indicators because other events may cause similar symptoms. And those moisture beetles are not the most reliable.

(This response would establish row C of table 6.1)

KE: What does it mean when the surge tank level is dropping slowly?

EXPERT: It is probably not a very small LOCA (type A) because a small drip would not affect system parameters at all. It tends to support a medium size break (type C).

(This response would establish the column associated with the surge level dropping in table 6.1.)

Of course, it is difficult to establish the precise confidence levels to be used in the table. Questions to the expert would help to define the numbers used, ranging from -100 for definitely no to +100 for definitely yes. However, once the table has been set, the rules can easily be implemented on a column-wise or row-wise basis. For instance, the rule regarding the surge tank level dropping is:

IF the surge level is dropping slowly

THEN the diagnosis is more likely to be a type C break and less likely to be a type A break

In the syntax of PERSONAL CONSULTANT PLUS:

IF:: SURGE__L = SLOW__DROP

THEN:: LOCA = LOCA__C CF 60 AND LOCA != LOCA__A CF 30

The full implementation is simply a collection of such rules (in any order) plus auxiliary information such as an imposed firing order (if desired) and display information. Typically, usable expert systems are limited to a few hundred rules.

It is impossible to predict the diagnosis in advance for all but the simplest systems. Thus, some "tuning" of the confidence factors has to be done. This may involve a comparison of the diagnoses to off-line simulations or station data. An alternative type of artificial intelligence, neural nets, are capable for learning or adapting. Neural net research has just begun at McMaster University, therefore it is not known to what degree this approach would aid in establishing a Reactor Operator Companion.

The above example (table 6.1) has been implemented in Personal Consultant Plus. This implementation plus explorations in neural nets can be viewed upon request at McMaster University.

CONCLUSION

The work completed to date shows that the overall concept appears sound and should be pursued. The simulator utilizing the rate form of the equation of state is efficient and robust. Future developments should include implementation of station control, thermal-hydraulic correlations and I/O interfacing. The trend analyzer should be implemented as discussed herein. The trend analyzer, simulator and expert system need to be integrated into a cohesive whole.

REFERENCES

- AN87 J. Anderson, Private Communication, 1987.
- GA86 W.J. Garland and J.D. Hoskins, "Approximate Functions for the Fast Calculation of Light Water Properties at Saturation", submitted to the International Journal of Multiphase Flow, July 1986.
- GA87a W.J. Garland, "A Comparison of the Rate Form of the Equation of State to the Jacobian Form", 13th Symposium on the Simulation of Reactor Dynamics and Plant Control, Chalk River Nuclear Laboratories, Chalk River, Canada, April 27-28, 1987.
- GA87b W.J. Garland and R. Sollychin, "The Rate Form of State for Thermalhydraulic Systems: Numerical Considerations", Engineering Computations, December 1987.
- HA84 L. Haar, J.S. Gallagher and G.S. Knell, "NBS/NRC Steam Tables: Thermodynamic and Transport Properties and Computer Programs for Vapour and Liquid States of Water in SI Units", Hemisphere Publishing Corporation, 1984.
- NA87 A. Natalizio, Private Communication, 1987.
- PO71 T.A. Porsching, J.H. Murphy and J.A. Redfield, "Stable Numerical Integration of Conservation Equations for Hydraulic Networks: Nuc. Sci. and Eng. 43, p. 218-225, (1971).

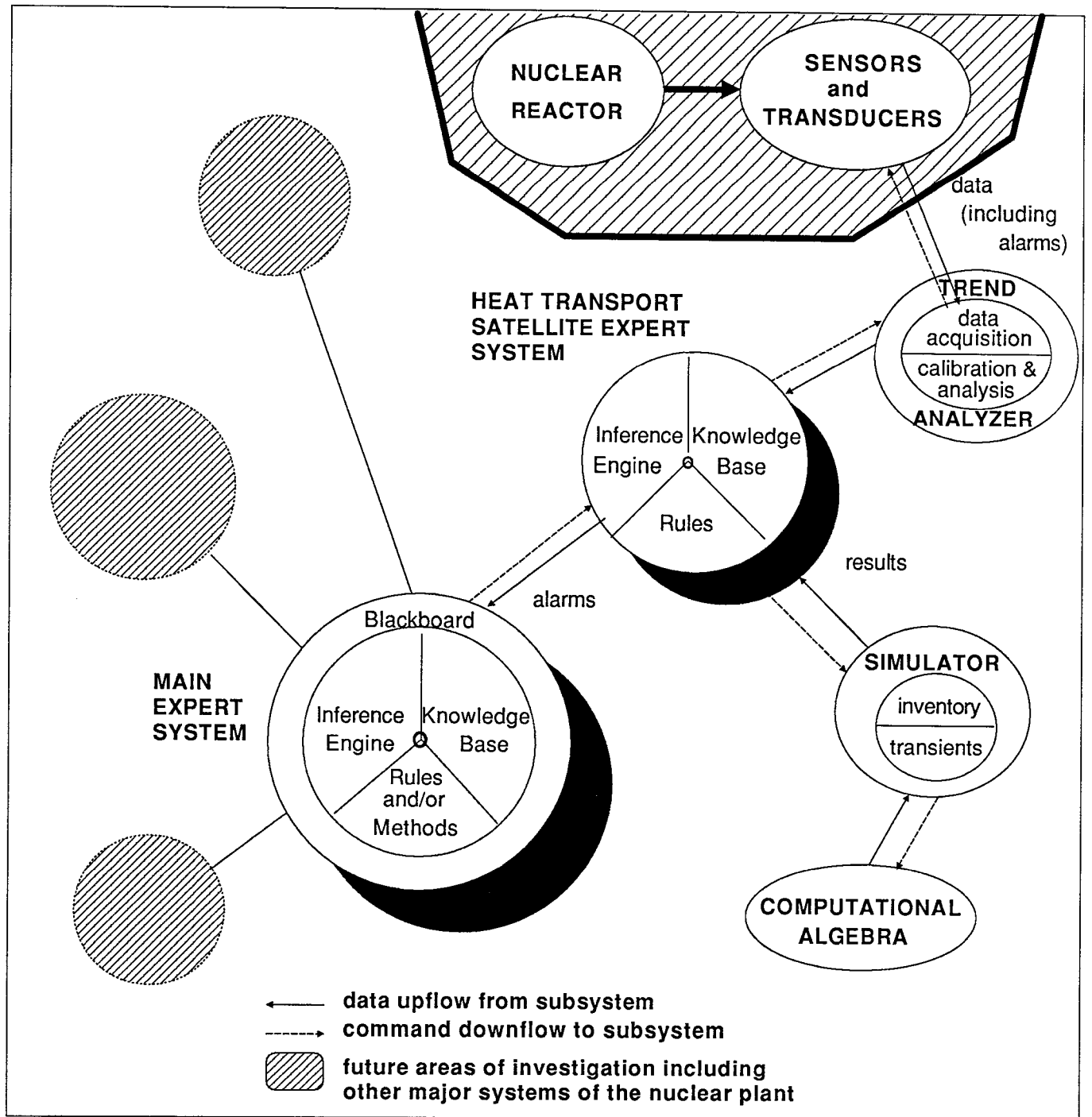


FIGURE 1.1 Current existing modules for the Operator Companion

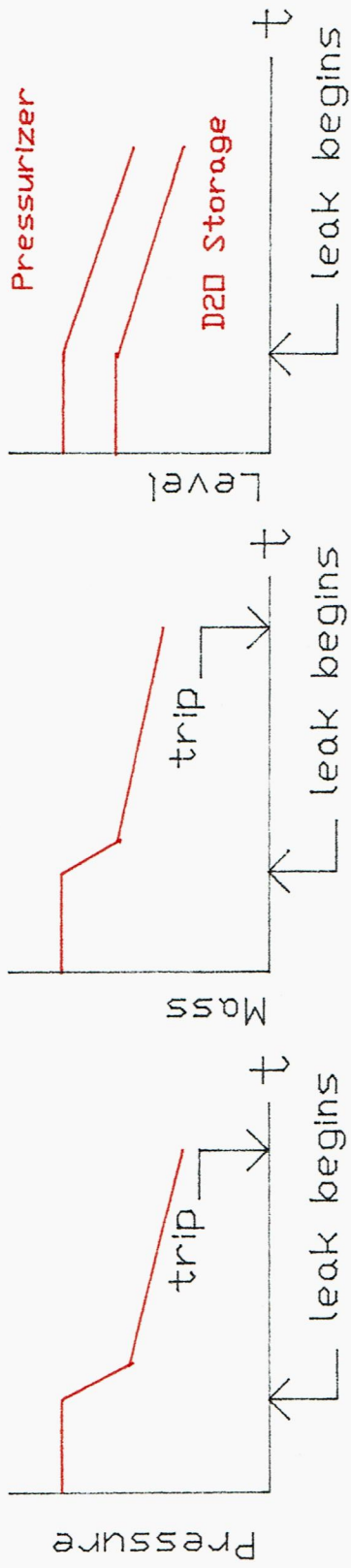


Figure 3.4 Category D Leakage Rate
 Feedpump Capacity $<$ RLEAK $<$ RMAX

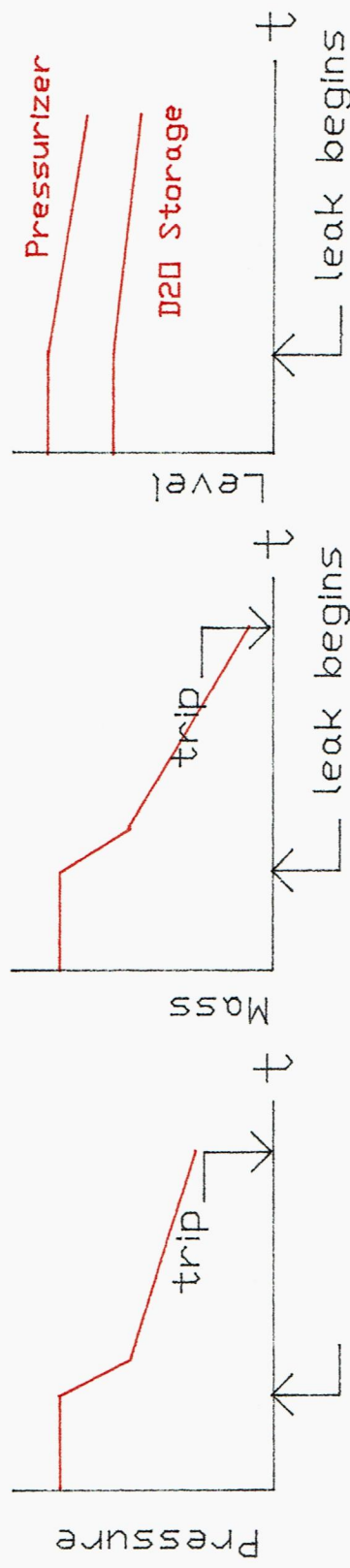


Figure 3.5 Category E Leakage Rate
 RLEAK $>$ RMAX

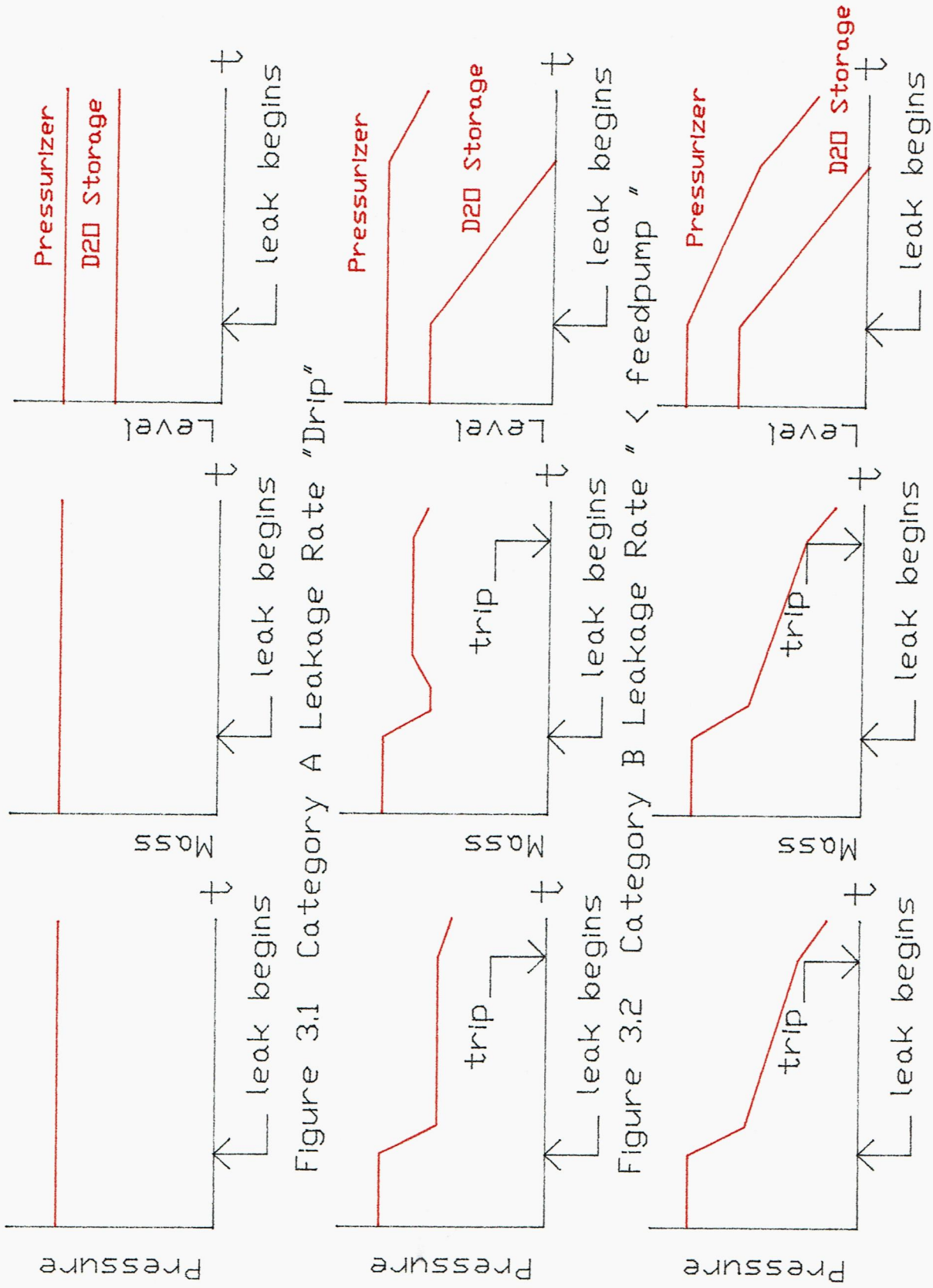


Figure 3.1 Category A Leakage Rate "Drip"

Figure 3.2 Category B Leakage Rate " $< feedpump$ "

Figure 3.3 Category C Leakage Rate " $> feedpump$ "

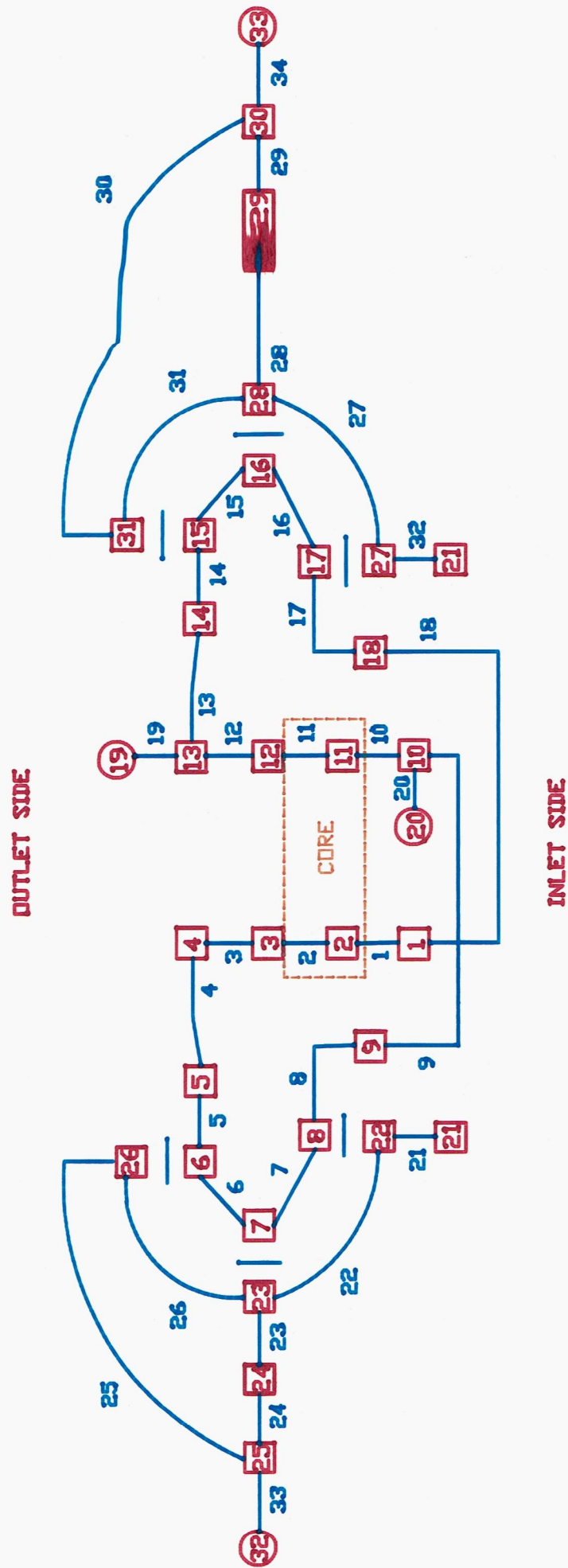
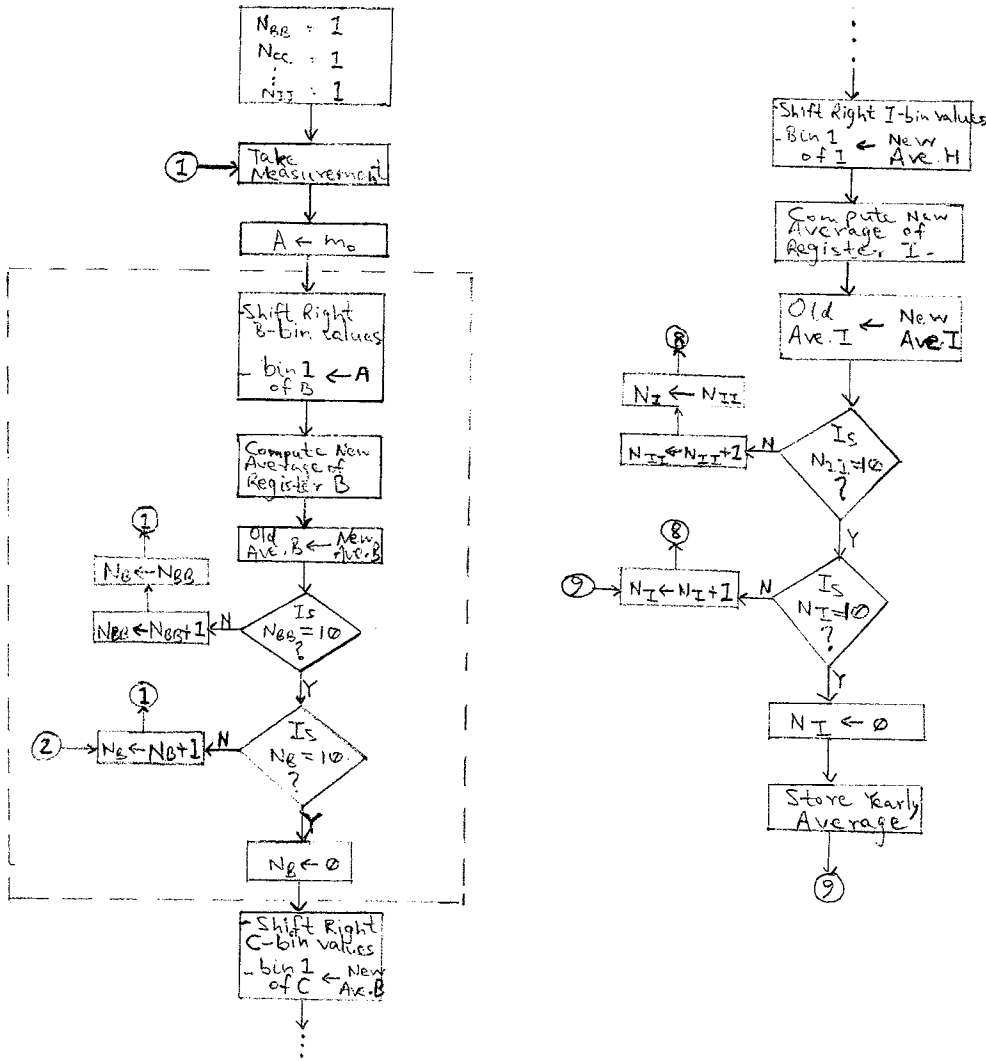


Figure 4.3 Nodal Layout of CANDU 300 Heat Transport System

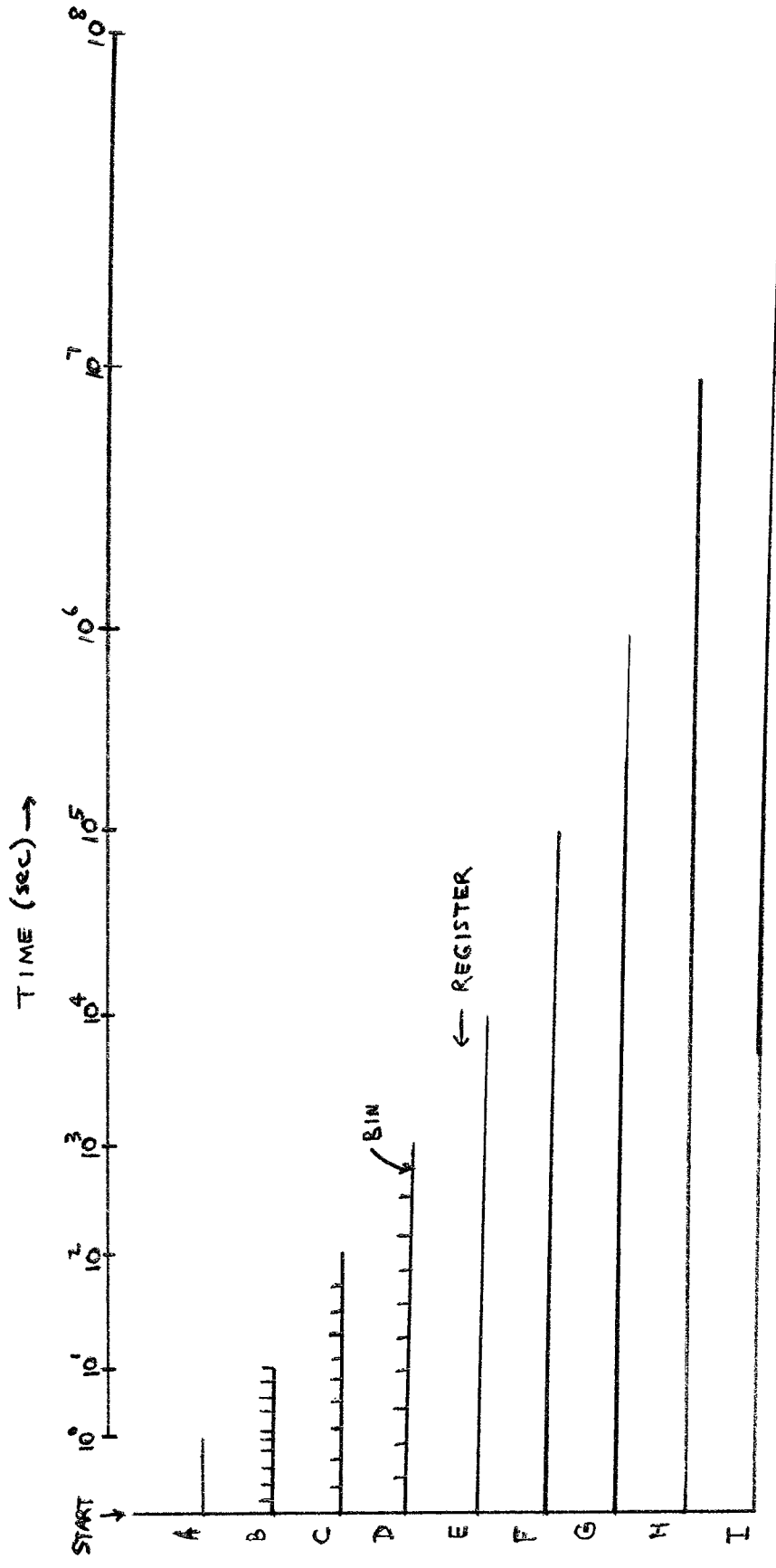


LEGEND: N_{jj} = No. of values in Register jj
for $jj = BB, CC, \dots, II$.
 N_j = Register Counter j ; $j = B, C, \dots, I$.
 OA_j = Old Average of Register j ;
for $j = B, C, \dots, I$.
 NA_j = New Average of Register j ;
for $j = B, C, \dots, I$.

NOTE: $NA_B = OA_B \left(\frac{N_{BB}-1}{N_{BB}} \right) + \frac{NA_A}{N_{BB}}$, etc.

where $NA_A = A = m_0$ since Register A only contains one value (only exception).

FIGURE 5.1 : FLOWCHART FOR COMPUTING MOVING AVERAGES



NOTE: Each REGISTER (excluding A) is divided into 10 BINS

FIGURE 5.2: DISTRIBUTION OF TIME SLICES